Using mouse-tracking data to visualise decision landscapes

Arkady Zgonnikov (arkady.zgonnikov@nuigalway.ie)
School of Psychology, National University of Ireland, Galway

Andrea Aleni (andrea.aleni@gmail.com)
Department of Electrical Engineering and Information Technology
University of Naples Federico II, Italy

Petri Piiroinen (petri.piiroinen@nuigalway.ie)
School of Mathematics, Statistics & Applied Mathematics
National University of Ireland, Galway

Denis O'Hora (denis.ohora@nuigalway.ie)
School of Psychology, National University of Ireland, Galway

Abstract

Computerised paradigms have enabled decision making researchers to gather rich data on human behaviour, including information on motor execution of a decision, e.g., by tracking mouse cursor trajectories. As the number and complexity of mouse-tracking studies rapidly increase, more sophisticated methodology is needed to analyse the decision trajectories. Here we present a new computational approach to generating decision landscape visualisations based on mouse-tracking data. Decision landscape is an analogue of energy potential field mathematically derived from velocity of mouse movement during a decision. Visualised as a 3D surface, it provides a comprehensive overview of motor evolution of decisions. Employing the dynamical systems theory framework, we develop a new method for generating decision landscapes based on arbitrary number of trajectories. The decision landscape visualisation have potential to become a novel tool for analysing mouse trajectories during decision execution, which can provide new insights into the dynamics of decision making.

Keywords: decision making; mouse tracking; dynamical systems; visualisation

Introduction

Traditionally, decision making studies have been focused on *what* people choose and explaining the mechanisms leading to the observed choice outcome distributions. Sequential sampling models (Busemeyer & Townsend, 1993; Ratcliff & Rouder, 1998) make predictions on the time required for the decision maker to arrive to a decision, thereby stimulating empirical research to measure response times in addition to choice outcomes. However, in the past decade, decision making researchers have been employing more advanced experimental paradigms, measuring behavioural activity during decision-making to investigate whether *how* we choose is meaningfully related to *what* we choose.

A variety of experimental methods have been used to study the cognitive processes underlying decision making. One class of paradigms, including eye tracking (Orquin & Loose, 2013) and different variations of information search paradigm (Payne, 1976), taps attentional processes, trying to answer the question of what information is attended to in the course of decision. Another strand of research, focused on *hand* or *mouse tracking*, examines how decisions are executed through motor system. These studies interpret motor output of a decision as a continuous trace of decisional processes. In a typical experiment on mouse tracking, the participant chooses between the two options presented in the corners of a computer screen (Fig. 1). The dynamics of the response, as expressed in recorded mouse cursor trajectories, can then reveal the degree of competition between the two options during choice.

Mouse (or hand) tracking have been employed to investigate decision making dynamics in a variety of different domains, e.g., speech processing (Spivey, Grosjean, & Knoblich, 2005), social categorisation (Freeman, Ambady, Rule, & Johnson, 2008; Freeman & Ambady, 2011), and intertemporal choice (Dshemuchadse, Scherbaum, & Goschke, 2013; O'Hora, Carey, Kervick, Crowley, & Dabrowski, 2016). The recent development of "off-the-shelf" solutions for capturing mouse cursor data (Freeman & Ambady, 2010; Kieslich, Wulff, Henninger, & Haslbeck, 2017) has further increased the amount and complexity of the data generated by mouse-tracking studies. However, the vast majority of available studies utilise only few basic measures derived from rich mouse-tracking data. At the same time, much potentially important information conveyed by mouse trajectories is still very often ignored. More advanced analysis methods can potentially enable us to get deeper insights from the rich data provided by the mouse-tracking paradigm.

Here we present a new computational approach for illustrating mouse-tracking data via three-dimensional visualisations of *decision landscape*. Recently, a method was suggested to infer such visualisations directly from the data (O'Hora, Dale, Piiroinen, & Connolly, 2013). Here, we build up on this work, employing an alternative, model-based approach. We assume that the decision process, as reflected by a mouse trajectory, is governed by a 'potential energy' landscape. The parameters defining the form of the landscape for each decision can then be fitted to capture specific mouse motion trajectory during that decision. Visualised as a 3D surface, this decision landscape provides a com-

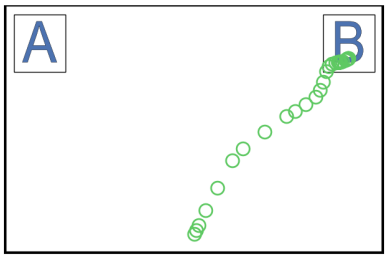

Figure 1: Typical setup of a mouse-tracking experiment. Plotted in green is an actual mouse trajectory representing binary choice in a learning task (O'Hora et al., 2013)

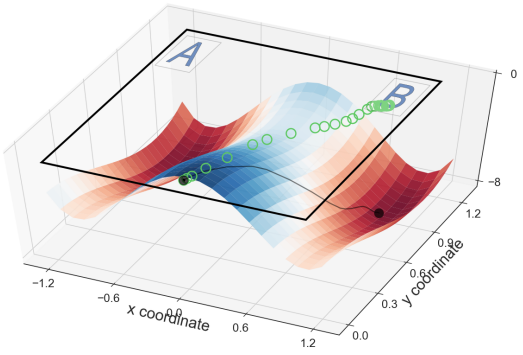

Figure 2: Mouse trajectory from Fig. 1 and a hypothetical decision landscape driving the decision process. The grey line is a projection of the trajectory on the decision landscape. The figure is based in part on visualisation of hypothetical decision attractor manifold by Spivey and Dale (2006).

prehensive overview of motor evolution of decisions. The suggested method can generate illustrations of decision landscapes based on arbitrary number of trajectories. Using previously collected data on a learning task (O'Hora et al., 2013), we demonstrate how decision landscape visualisations can be used to compare sets of mouse trajectories between experimental conditions or individual decision makers in a comprehensive, visually appealing way.

Visualising decision landscape

The proposed method is aimed at reconstructing a 3D decision landscape based on a mouse trajectory of a decision (or a set of trajectories). We assume that each trajectory can be described by a dynamical system of a specific form, which incorporates a parametrised function describing the shape of the two-well landscape. By fitting this dynamical system to a set of trajectories, we obtain specific values of the parameters characterising these particular trajectories. We can then use these parameters to generate the 3D visualisation of the decision landscape characterising all of the given decisions. The source code implementing all the procedures of the method in Python is available via Open Science Framework (Zgonnikov, Aleni, Piiroinen, O'Hora, & di Bernardo, 2017).

Data requirements and preprocessing

To visualise decision landscapes, we use two-dimensional trajectories obtained in a typical mouse-tracking experiment (Fig. 1). We assume that each decision trajectory starts in the bottom centre part of the screen and ends in either top left or top right corner. The method can be generalised to the case of more than two choice options; with minor adjustments (e.g., using two-dimensional projections of 3D trajectories) it can as well be used with any other experimental paradigm generating simple enough continuous trajectories, for instance, arm reaching (Song & Nakayama, 2008; Gallivan & Chapman, 2014).

Importantly, the current version of the method assumes continuity and smoothness of the trajectories, which is not always the case. In a fraction of experimental trials, participants change their mind in the course of a trial, which is indicated by major shifts in the x-direction of a decision trajectory (Resulaj, Kiani, Wolpert, & Shadlen, 2009; Freeman, 2014). The deterministic dynamical model of a decision trajectory utilised in the present method does not account for such changes-of-mind, so we recommend using the method only with the trajectories without abrupt shifts.

As screen size and proportions can differ between experiments, we illustrate the method for spatially normalised trajectories. In particular, the screen coordinates are assumed to be rescaled such that each trajectory originates near $(x,y) = (0,0)$ and ends in the vicinity of $(x,y) = (-1,1)$ (left target) or $(x,y) = (1,1)$ (right target).

Each trajectory is supposed to be described by the time series of x- and y-coordinates of the mouse cursor on the screen. In addition to this data, the method also requires x- and y-velocities of the mouse cursor at each time step, which are computed numerically.

Model of trajectory dynamics

Without aiming at developing a model *explaining* the dynamics of a decision, we use a simple dynamical system to *describe* the decision trajectory, capturing the high-level features of motion of the mouse cursor. We describe the time dependent x- and y-components of a decision trajectory by a system of ordinary differential equations

$$\begin{aligned} \tau\dot{x} &= -\frac{\partial V}{\partial x}, \\ \tau\dot{y} &= -\frac{\partial V}{\partial y}, \end{aligned} \tag{1}$$

where $\dot{x} = \frac{\mathrm{d}x}{\mathrm{d}t}$ and $\dot{y} = \frac{dy}{dt}$ are the time derivatives of x and y, $\tau > 0$ is the time scale parameter expressed in seconds, $V(x,y)$ is a function describing the decision landscape, which defines the dynamics of the system, and $\frac{\partial V}{\partial x}$ and $\frac{\partial V}{\partial y}$ are its partial derivatives with respect to x and y.

Our method is not constrained by some particular function $V(x,y)$; here we use one of the simplest possible variants. We assume that $V(x,y)$ comprises a fixed baseline component

$V_x(x) + V_y(y)$ and a parametrised component $V_{xy}(x, y)$ so that

$$V(x,y) = V_x(x) + V_y(y) + V_{xy}(x,y), \tag{2}$$

where $V_x(x)$ and $V_y(y)$ are polynomials chosen in a way that the two target locations, (-1, 1) and (1, 1), are attracting steady states ("attractors"), and the starting location (0, 0) is a repelling state of the system (1) given that $V_{xy}(x, y) \equiv 0$. Thus,

$$V_x(x) = \int \frac{\partial V_x}{\partial x}\,\mathrm{d}x = \int x(x+1)(x-1)\,\mathrm{d}x = \frac{x^4}{4} - \frac{x^2}{2}, \tag{3}$$

$$V_y(y) = \int \frac{\partial V_y}{\partial y}\,\mathrm{d}y = \int y(y-1)\,\mathrm{d}y = \frac{y^3}{3} - \frac{y^2}{2}. \tag{4}$$

Having a two-attractor decision landscape as a baseline, we introduce the parametrised polynomial component $V_{xy}(x,y)$ to be able to account for asymmetry in the landscape and other, more intricate properties of experimental trajectories. Here, also for the reason of simplicity, for $V_{xy}(x,y)$ we use a polynomial function of x and y

$$V_{xy}(x,y) = \sum_{k=2}^{\alpha} \sum_{\substack{i,\,j>0 \\ i+j=k}} c_{ij} x^i y^j / (k-1), \tag{5}$$

where the parameter $\alpha \geq 2$ determines the number of terms in the polynomial, which in turn regulates flexibility of the model, and the coefficients c_{ij} are fitted to the data. Note that with increasing α the number of free parameters increases, thus the fitted values of these parameters may be difficult to interpret for large α. We recommend using the method with $\alpha = 2$, 3, or 4, depending on the complexity of the trajectories, and to take into account the trade-off between approximation accuracy and interpretability of the parameters.

The effect of the model parameters τ and c_{ij} on the shape of the decision landscape can be analysed independently of the experimental data (Fig. 3). For any α, two parameters always enter the model, τ and c_{11}. The parameter τ affects the characteristic time scale of the system motion: the larger the value of τ, the slower the motion of the mouse generated by the model (in both directions). In what follows we use the baseline value $\tau = 0.05$ s.

The parameter c_{11}, corresponding to the only second-order polynomial term of the model, is the primary determinant of the asymmetry of the decision landscape. Such asymmetry may be caused, for instance, by strong prevalence of one decision outcome over the other. Another possible example of asymmetry would be a situation when the trajectories towards one option are consistently faster compared to the trajectories pointing to the other option, with the two options being chosen equally likely.

When $\alpha \geq 3$, additional polynomial terms enter $V_{x,y}(x,y)$. The effects of the parameters c_{ij} in front of these higher-order terms are somewhat similar to those of τ and c_{11}, but allow for much finer tuning of the decision landscape to the experimental trajectories.

Fitting the model to the single trajectory

For a single experimental trajectory, we aim to find the parameters allowing the model (1)–(5) to reproduce this trajectory as closely as possible. We can define the fitting error in two ways: as a function of the positional difference between the data and the modelled trajectory, or based on the difference in mouse velocities between the data and the model. The first approach would result in a more accurate approximation of trajectories, but requires substantially more computational time, as on each step of the fitting algorithm the system of differential equations (1) has to be integrated numerically. The second approach, employing the velocity-based fitting error, is much more efficient in terms of computational resources, sometimes at the expense of approximation accuracy. Here we focus on the latter; the supplied source code implements both approaches.

Given an experimental mouse trajectory sampled at m time steps and the numerically derived mouse velocities $\{v_x^{\text{data}}, v_y^{\text{data}}\}$, we define the fitting error

$$H(\tau, c_{ij}, \{v_x^{\text{data}}, v_y^{\text{data}}\}) = \frac{1}{m}\sum_{i=0}^{m} (v_x^{\text{model}}(x_i,y_i) - v_x^{\text{data}}(t_i))^2 + (v_y^{\text{model}}(x_i,y_i) - v_y^{\text{data}}(t_i)), \tag{6}$$

where $v_{x,y}^{\text{model}}(x_i,y_i)$ are the values of the right-hand side of the system (1) computed at each point (x_i,y_i) along the experimental trajectory. These values depend on the current parametrisation of the model, so the defined error function depends both on the model parameter values and the experimental trajectory.

Using numerical optimisation routines (available, e.g., in the Python package `scipy.optimize`), one can find the values of the model parameters τ, c_{ij} minimising function (6) for a given mouse trajectory. These parameters are substituted in Eq. (5), which, along with Eqs. (2)–(4), fully specifies $V(x,y)$. The 3D plot of the function $V(x,y)/\tau$ then visualises the decision landscape representing the original trajectory.

Fitting to multiple trajectories

Visualising a decision landscape that would integrate the properties of multiple trials (within a single experimental condition, individual participant, or a group of participants) is where the method can prove most useful. To be able to do this, we use the same approach as in the case of a single trial, and minimise the average error across individual trials in a set of trials. Given the set of N trajectories and their velocities $\{v_x^{\text{data}}, v_y^{\text{data}}\}_{n=1}^N$, the fitting error for multiple trajectories is defined by

$$\hat{H}(\tau, c_{ij}, \{v_x^{\text{data}}, v_y^{\text{data}}\}_{n=1}^N) = \frac{1}{N}\sum_{n=1}^{N} H(\tau, c_{ij}, \{v_x^{\text{data}}, v_y^{\text{data}}\}_n), \tag{7}$$

where H is defined in (6).

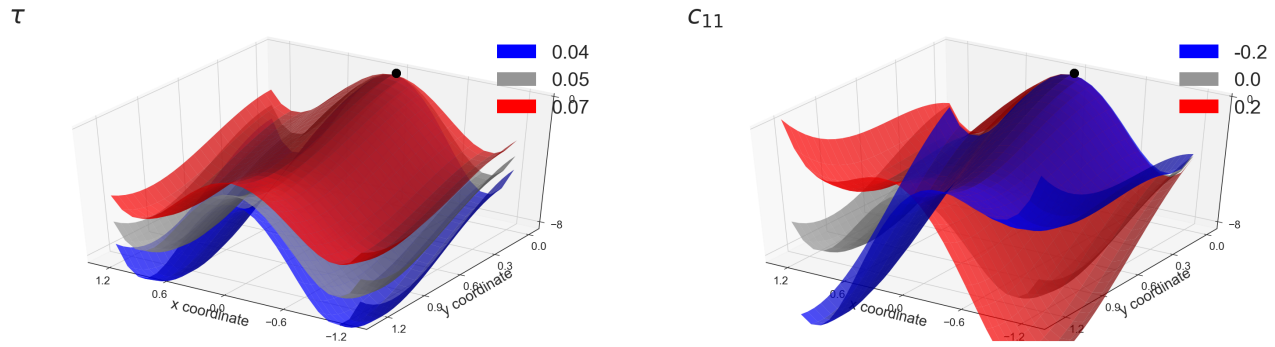

Figure 3: Changes in the baseline decision landscape depending on the parameters of the model for $\alpha = 2$. In each panel, all parameters except for the one in the panel title are fixed at the baseline levels $\tau = 0.05$, $c_{i,j} = 0$; the baseline landscape is shown in grey colour. In this and the following figures, the black marble marks the starting location of a trial.

Example scenarios

We illustrate several potential scenarios of using our method to visualise mouse tracking data by applying it to the previously obtained experimental data on a simple learning task (O'Hora et al., 2013). The task consisted of a series of binary choices between abstract symbols, with each symbol yielding either low or high reward (e.g., 5 or 20 points). The goal of the participants was to get as many points as possible throughout a set of 36 trials, which included low vs. low, high vs. low, and high vs. high choices. By the end of the experiment, most of the participants successfully learned to choose only the symbols associated with high reward.

Here we only consider part of the dataset corresponding to high vs. low choices, so that there is always a "correct" choice. The data are preprocessed so that the correct ("high") option is mapped to right-hand corner of the screen, and incorrect option is located in the left-hand corner. To fit the experimental data, we used the version of the model with $\alpha = 4$, which has seven free parameters. The baseline values of the parameters were set to $\tau = 0.05$, $c_{ij} = 0$.

Fig. 4 shows the example decision landscapes obtained for three trajectories generated by Participant 444. The shape of the fitted landscape changes depending on the dynamics of the decision. Two key properties of a mouse trajectory reflected by the fitted decision surface are: *motion time*, i.e., the how long it takes for the cursor to reach the response area once it leaves the starting location, and *maximum deviation* of the trajectory from the ideal, straight-line trajectory (termed "max-d").

Importantly, the decision landscape is supposed to capture dynamics rather than geometry of the mouse trajectory. However, with increasing deviation of the trajectory towards unchosen option, the strength of the attractor corresponding to that option increases. Moreover, in extreme cases, when deviation towards competitor option is very large, the attractor representing the unchosen option can be even stronger than the attractor corresponding to the eventually chosen option (yellow surface in Fig. 4). This situation, paradoxically indicating that the attraction towards the unchosen option during

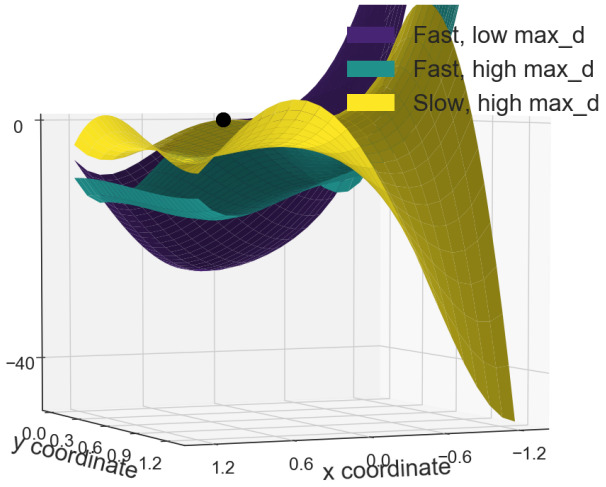

Figure 4: Decision landscapes of three representative trials of Participant 444. In all three trials, the subject had chosen the option on the right ("correct choice"). Trial 2 (yellow surface) was slow (motion time 0.72 s) and mildly conflicted (max-d 0.23). In trial 15 (purple surface), the mouse trajectory was fast (motion time 0.15 s) and was close to straight line (max-d 0.02). In trial 28 (green surface), the trajectory was still relatively fast (motion time 0.37 s), but substantially curved towards the unchosen option (max-d 0.77).

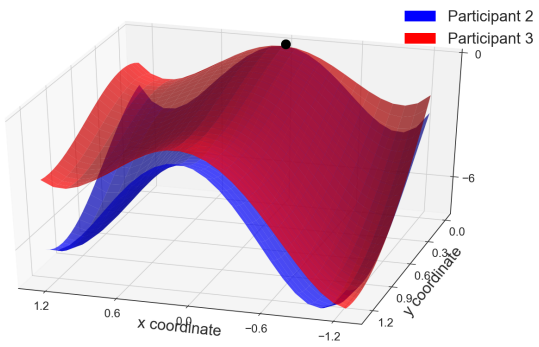

Figure 5: Decision landscapes of the two representative participants. Participant 2 (blue surface) had chosen right- and left-hand-side options 7 times each (mean motion times 0.56 and 0.45 s). Red surface illustrates Participant 3 with the right-hand-side option chosen 3 times (mean motion time 0.5 s) and the left-hand-side option chosen 10 times (mean motion time 0.4 s).

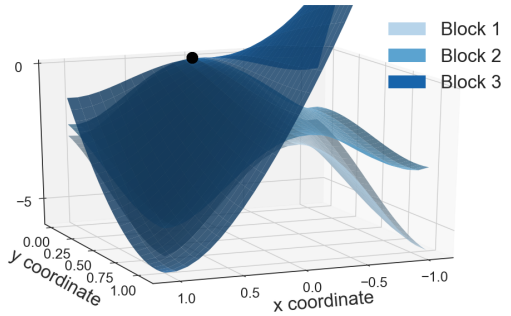

Figure 6: Evolution of decisions of Participant 4 throughout three consecutive blocks of trials. Each surface corresponds to all trials of a block.

the trial was stronger than towards the chosen one, is very rare and happens only for landscapes of individual trajectories with high max-d.

One of the potential applications of the present method is highlighting individual differences between two participants performing the same task. To do this, one needs to obtain decision landscapes individually for each participant by fitting the model to all trials of that individual simultaneously. In the case of multiple-trajectory fitting, the fitting error is defined as the average error across all trajectories of a given participant, so the resulting decision landscape will integrate the information on how often and how fast each option was chosen, providing a comprehensive overview of the participant's decisions throughout the experiment.

We illustrate this by comparing the decision landscapes of the two participants (Fig. 5). Participant 2 was equally likely to chose either option, with faster trajectories reaching towards the incorrect (left-hand-side) option. Participant 3 had chosen the incorrect (left) response more often, and it was chosen on average faster than the correct option.

If the experimental task involves adaptation, the current method can be used to highlight learning patterns within subjects. Fig. 6 represents three decision landscapes separately fitted to the trajectories of three consecutive blocks of trials of Participant 4 (with each block containing six to eight trials). The decision surface gradually changes from the two-attractor landscape slightly favouring the right attractor to the single-attractor configuration, thereby tracking the learning-induced evolution of preference across blocks.

Discussion

The decision landscape visualisations provide comprehensive overview of a mouse-tracking data. Each visualisation integrates the information on 1) the likelihood of each option to be chosen, 2) the duration of the response, and 3) the degree of competition between the options.

The first attempt to develop an algorithm to visualise decision landscapes based on mouse tracking data has been recently made by O'Hora et al. (2013). Their approach, however, is purely data-driven, and thus requires hundreds of trajectories to generate a reliable visualisation of the decision surface. By incorporating prior assumptions about decision landscape $V(x,y)$ into a parametrised model, we dramatically reduce the data requirements of our method. As demonstrated above, the method proposed here can be used with as few trajectories as one, but can also incorporate arbitrary number of trajectories.

One of the main limitations of the proposed method is its focus on trajectories without changes-of-mind. An important (although relatively rare) class of decisions are those involving preference reversals during choice execution. These happen even in simple perceptual discrimination tasks (Resulaj et al., 2009); in more cognitively demanding tasks the frequency of changes-of-mind can increase up to 20% (Freeman, 2014). Developing a way of visualising decision landscapes of the change-of-mind trajectories is one of our foremost future research directions.

Attractor models have proved useful in understanding *outcomes* of cognitive processes such as categorisation (Tuller, Case, Ding, & Kelso, 1994), risky decision making (van Rooij, Favela, Malone, & Richardson, 2013), and binary decision making in intermittent motor control (Zgonnikov & Lubashevsky, 2015). This work is among the first attempts to apply the concepts of dynamical systems theory to *process* data characterising decisions. We hope that the proposed decision landscape visualisation approach will eventually grow in a new tool for analysing decision trajectories, which will be able to provide new insights into dynamics of decision making.

Acknowledgements

This work was supported in part by Government of Ireland Postdoctoral Fellowship GOIPD/2015/481.

References

Busemeyer, J. R., & Townsend, J. T. (1993). Decision field theory: a dynamic-cognitive approach to decision making in an uncertain environment. *Psychological review*, *100*(3), 432.

Dshemuchadse, M., Scherbaum, S., & Goschke, T. (2013). How decisions emerge: Action dynamics in intertemporal decision making. *Journal of Experimental Psychology: General*, *142*(1), 93.

Freeman, J. B. (2014). Abrupt category shifts during real-time person perception. *Psychonomic bulletin & review*, *21*(1), 85–92.

Freeman, J. B., & Ambady, N. (2010). MouseTracker: Software for studying real-time mental processing using a computer mouse-tracking method. *Behavior Research Methods*, *42*(1), 226–241.

Freeman, J. B., & Ambady, N. (2011). A dynamic interactive theory of person construal. *Psychological review*, *118*(2), 247.

Freeman, J. B., Ambady, N., Rule, N. O., & Johnson, K. L. (2008). Will a category cue attract you? Motor output reveals dynamic competition across person construal. *Journal of Experimental Psychology: General*, *137*(4), 673.

Gallivan, J. P., & Chapman, C. S. (2014). Three-dimensional reach trajectories as a probe of real-time decision-making between multiple competing targets. *Frontiers in Neuroscience*, *8*.

Kieslich, P. J., Wulff, D. U., Henninger, F., & Haslbeck, J. M. B. (2017). *Mousetrap: An R package for processing and analyzing mouse-tracking data.* Retrieved from `https://doi.org/10.5281/zenodo.290283` doi: 10.5281/zenodo.290283

O'Hora, D., Carey, R., Kervick, A., Crowley, D., & Dabrowski, M. (2016). Decisions in Motion: Decision Dynamics during Intertemporal Choice reflect Subjective Evaluation of Delayed Rewards. *Scientific Reports*, *6*, 20740.

O'Hora, D., Dale, R., Piiroinen, P. T., & Connolly, F. (2013). Local dynamics in decision making: The evolution of preference within and across decisions. *Scientific reports*, *3*, 2210.

Orquin, J. L., & Loose, S. M. (2013). Attention and choice: A review on eye movements in decision making. *Acta psychologica*, *144*(1), 190–206.

Payne, J. W. (1976). Task complexity and contingent processing in decision making: An information search and protocol analysis. *Organizational behavior and human performance*, *16*(2), 366–387.

Ratcliff, R., & Rouder, J. N. (1998). Modeling response times for two-choice decisions. *Psychological Science*, *9*(5), 347–356.

Resulaj, A., Kiani, R., Wolpert, D. M., & Shadlen, M. N. (2009). Changes of mind in decision-making. *Nature*, *461*(7261), 263–266.

Song, J.-H., & Nakayama, K. (2008). Numeric comparison in a visually-guided manual reaching task. *Cognition*, *106*(2), 994–1003.

Spivey, M. J., & Dale, R. (2006). Continuous dynamics in real-time cognition. *Current Directions in Psychological Science*, *15*(5), 207–211.

Spivey, M. J., Grosjean, M., & Knoblich, G. (2005). Continuous attraction toward phonological competitors. *Proceedings of the National Academy of Sciences of the United States of America*, *102*(29), 10393–10398.

Tuller, B., Case, P., Ding, M., & Kelso, J. (1994). The nonlinear dynamics of speech categorization. *Journal of Experimental Psychology: Human Perception and Performance*, *20*(1), 3.

van Rooij, M. M., Favela, L. H., Malone, M., & Richardson, M. J. (2013). Modeling the Dynamics of Risky Choice. *Ecological Psychology*, *25*(3), 293–303.

Zgonnikov, A., Aleni, A., Piiroinen, P. T., O'Hora, D., & di Bernardo, M. (2017, Mar). *Visualising decision landscapes using mouse-tracking data.* Open Science Framework. Retrieved from `https://osf.io/5q364/`

Zgonnikov, A., & Lubashevsky, I. (2015). Double-well dynamics of noise-driven control activation in human intermittent control: the case of stick balancing. *Cognitive Processing*, *16*(4), 351–358.